

See discussions, stats, and author profiles for this publication at: <https://www.researchgate.net/publication/230717979>

Explanation of Deuterium and Muonium Kinetic Isotope Effects for Hydrogen Atom Addition to an Olefin

ARTICLE in JOURNAL OF THE AMERICAN CHEMICAL SOCIETY · NOVEMBER 1998

Impact Factor: 12.11 · DOI: 10.1021/ja982616i

CITATIONS

15

READS

10

5 AUTHORS, INCLUDING:



Jordi Villà-Freixa

University of Vic - Central University of Catal...

90 PUBLICATIONS 1,983 CITATIONS

SEE PROFILE



Jose C Corchado

Universidad de Extremadura

118 PUBLICATIONS 3,296 CITATIONS

SEE PROFILE



Angels Gonzalez-Lafont

Autonomous University of Barcelona

119 PUBLICATIONS 1,992 CITATIONS

SEE PROFILE



José M Lluch

Autonomous University of Barcelona

270 PUBLICATIONS 4,266 CITATIONS

SEE PROFILE

Explanation of Deuterium and Muonium Kinetic Isotope Effects for Hydrogen Atom Addition to an Olefin

Jordi Villà,^{†,‡} José C. Corchado,^{‡,§} Angels González-Lafont,[†]
José M. Lluch,[†] and Donald G. Truhlar^{*,‡}

Departament de Química
Universitat Autònoma de Barcelona
08193 Bellaterra, Barcelona, Spain

Department of Chemistry and Supercomputer Institute
University of Minnesota
Minneapolis, Minnesota 55455-0431

Departamento de Química Física
Universidad de Extremadura
06071, Badajoz, Spain

Received July 24, 1998

Recently, several experimental^{1–3} and theoretical^{4,5} papers have reassessed the kinetics of the gas-phase hydrogen atom addition to the ethylene molecule, which is a prototype for the general case of addition of a free radical to a multiple bond. Theoretical work by Hase et al.⁴ and ourselves⁵ has established two conclusions about the dynamics of this reaction. (1) The reaction shows statistical behavior, so that the generalized transition state theory and the Rice–Ramsperger–Kassel–Marcus theory can simultaneously fit the rates of the C₂H₄ + H addition and the C₂H₅ unimolecular dissociation. (2) The transition state for the reaction is loose. We showed that it is necessary to consider the temperature dependence of the location of the transition state (using variational transition state theory,⁶ VTST) to overcome the limitations of previous calculations which employed static transition states (based on conventional transition state theory which assumes an identical geometry for the transition state at all temperatures). The major difficulty in describing the dynamics is to obtain a reliable potential energy surface. This was accomplished in ref 5 by introducing a new method to (in principle) extrapolate electronic structure calculations to the limit of full configuration mixing and a complete one-electron basis set. This method, called variable scaling of external correlation (VSEC), is based on the previously described scaled external correlation⁷ (SEC) method. VSEC uses a geometry-dependent scale factor, $F(R)$ where R is some distinguished reaction coordinate,⁸ to combine a complete-active-space self-consistent-field⁹ (CASSCF) calculation with a calculation including an appreciable amount of the dynamical correlation energy. The function $F(R)$ contains three parameters that are fitted in order to

obtain VTST rate constants that fit the experimental rates for the protium addition.

Attempts to explain deuterium kinetic isotope effects (KIEs) for the H + C₂H₄ reaction by means of ab initio electronic structure calculations combined with conventional transition state calculations have been unsuccessful.^{10,11} The very poor agreement of the theoretical and experimental KIEs raised questions about the validity of the Born–Oppenheimer approximation and the other assumptions of transition state theory.¹¹ An even greater challenge to theory that has also gone unmet has been provided by the results of Garner et al.,¹ who applied the muon spin rotation technique¹² to Mu + C₂H₄, to directly measure the pressure-independent (i.e., high-pressure) addition rate constant k_a . KIEs involving muonium (Mu) are very sensitive to the correct inclusion of quantum effects since the muonium atom (the isotope of hydrogen with a positive muon as its nucleus) is 8.8 times lighter than protium (H).¹³ Encouraged by our success⁵ for the protium addition, we have now examined the question of whether a consistent theoretical explanation of the KIEs for this prototype addition reaction is finally possible.

Geometries and vibrational frequencies were calculated for stationary points (reactants, product, and saddle point) using quadratic configuration interaction with single and double excitations¹⁴ (QCISD) and the 6-311G(d,p)¹⁵ basis set. At the same level of theory a distinguished-coordinate path⁸ (DCP) was constructed by following an isotope-independent distinguished coordinate R , which was taken to be the C–H separation distance of the attacking hydrogen. After evaluating the first and second derivatives at 21 points on the DCP, the reorientation-of-the-dividing-surface (RODS) algorithm¹⁶ was used to variationally optimize the generalized transition-state dividing surfaces. The resulting generalized transition state geometries, gradients, and Hessians were rotated into a consistent orientation by the Chen algorithm,¹⁷ and generalized normal-mode vibrational frequencies and reaction-path curvature components and the zero-point energy (ZPE) were calculated at each point. The vibrational calculations were based on redundant curvilinear coordinates.¹⁸ Energies along the reaction path were then corrected by means of the VSEC approximation⁵ with the external correlation energy estimated by the coupled cluster approximation with single and double excitations and a perturbative treatment of connected triple excitations,¹⁹ CCSD(T), again with the 6-311G(d,p) basis. The parameters of the $F(R)$ function were optimized in order to reproduce the experimental rate constants for the protium addition. Reaction-path data were obtained all along the reaction path by the mapped interpolation²⁰ algorithm. The resulting barrier height, 1.7 kcal/mol, is 0.5 kcal/mol higher than the value in ref 4.

Pressure-independent rate constants were calculated as functions of temperature T by canonical variational transition state theory⁶

[†] Universitat Autònoma de Barcelona.

[‡] University of Minnesota.

[§] Universidad de Extremadura.

(1) Garner, D. M.; Fleming, D. G.; Arseneau, D. J.; Senba, M.; Reid, I. D.; Mikula, R. J. *J. Chem. Phys.* **1990**, *93*, 1732.

(2) Hanning-Lee, M. A.; Green, N. J. B.; Pilling, M. J.; Robertson, S. H. *J. Phys. Chem.* **1993**, *97*, 860.

(3) Feng, Y.; Niiranen, J. T.; Bencsura, Á.; Knyazev, V. D.; Gutman, D.; Tsang, W. J. *J. Phys. Chem.* **1993**, *97*, 871.

(4) Hase, W. L.; Schlegel, H. B.; Balbyshev, V.; Page, M. *J. Phys. Chem.* **1996**, *100*, 5354; **1997**, *101*, 5026(E).

(5) Villà, J.; González-Lafont, A.; Lluch, J. M.; Truhlar, D. G. *J. Am. Chem. Soc.* **1998**, *120*, 5559.

(6) (a) Truhlar, D. G.; Isaacson, A. D.; Garrett, B. C. In *Theory of Chemical Reaction Dynamics*; Baer, M., Ed.; CRC Press: Boca Raton, FL, 1985; Vol. 4, p 65. (b) Truhlar, D. G.; Garrett, B. C.; Klippenstein, S. J. *J. Phys. Chem.* **1997**, *100*, 112771.

(7) Brown, F. B.; Truhlar, D. G. *Chem. Phys. Lett.* **1985**, *117*, 307.

(8) See, for example: (a) Steckler, R.; Truhlar, D. G. *J. Chem. Phys.* **1990**, *93*, 6570. (b) Heidrich, D. In *The Reaction Path in Chemistry*; Heidrich, D., Ed.; Kluwer: Dordrecht, 1995.

(9) Roos, B. O.; Taylor, P. R.; Siegbahn, P. E. M. *Chem. Phys.* **1980**, *48*, 152.

(10) Nagase, S.; Fueno, T.; Morokuma, K. *J. Am. Chem. Soc.* **1979**, *101*, 5849.

(11) (a) Sugawara, K.; Okazaki, K.; Sato, S. *Chem. Phys. Lett.* **1981**, *78*, 259. (b) Sugawara, K.; Okazaki, K.; Sato, S. *Bull. Chem. Soc. Jpn.* **1981**, *54*, 2872.

(12) Claxton, T. A. *Chem. Soc. Rev.* **1995**, 437.

(13) Walker, D. C. *J. Chem. Soc., Faraday Trans.* **1998**, *94*, 1.

(14) Pople, J. A.; Head-Gordon, M.; Raghavachari, K. *J. Chem. Phys.* **1987**, *87*, 5968.

(15) Krishnan, R.; Binkley, J. S.; Seeger, R.; Pople, J. A. *J. Chem. Phys.* **1980**, *72*, 650.

(16) Villà, J.; Truhlar, D. G. *Theor. Chem. Acc.* **1997**, *97*, 317.

(17) Chen, Z. *Theor. Chim. Acta* **1989**, *75*, 481.

(18) Chuang, Y.-Y.; Truhlar, D. G. *J. Chem. Phys.* **1997**, *107*, 83.

(19) Raghavachari, K.; Trucks, G. W.; Pople, J. A.; Head-Gordon, M. *Chem. Phys. Lett.* **1989**, *157*, 479.

(20) Corchado, J. C.; Coitiño, E. L.; Chuang, Y.-Y.; Fast, P.; Truhlar, D. G. *J. Phys. Chem. A* **1998**, *102*, 2424.

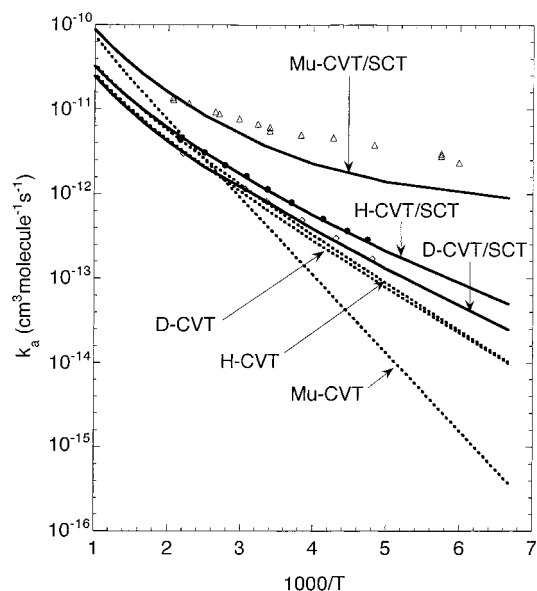


Figure 1. Arrhenius plots for the CVT (dashed lines) and the CVT/SCT (solid lines) calculations for the $X + \text{C}_2\text{H}_4$ addition, with $X = \text{Mu}$, H , and D . Also shown are the experimental data for these reactions (Mu , open triangles; H , solid circles; D , open diamonds).

(CVT) with multidimensional tunneling contributions calculated by the small-curvature tunneling²¹ (SCT) approximation.

Figure 1 is an Arrhenius plot for the three isotopic variants of the reaction. The experimental results have been taken from Sugawara et al.¹¹ for H and D addition and from Garner et al.¹ for muonium addition. Theoretical results are shown for CVT without tunneling and for CVT/SCT.

Without tunneling, the Mu rate constants are calculated to be 7 times smaller than the H ones and 6 times smaller than the D ones at 200 K, whereas experimentally they are larger. Figure 1 shows that including tunneling gives the correct trend.²² At 461 K, the highest T for which the KIEs are available, k_{Mu} and k_{H} are computed to be within a factor of 1.2 of each other without tunneling, whereas when tunneling is included $k_{\text{Mu}}/k_{\text{H}} = 2.7$, in excellent agreement with the experimental ratio of 2.8. (The tunneling effect can be even larger for other Mu reactions.²³) Thus, tunneling plays a dominant role in getting the correct trends for Mu . Figure 1 shows that tunneling also explains the KIE for D . As an example, at 230 K, tunneling increases the rate constant by factors of 35, 2.0, and 1.5 for Mu , H , and D , respectively. The fact that tunneling depends sensitively on the variation of the potential energy and ZPE over an appreciable portion of the reaction path (in particular the part of the reaction path with $\text{C}-\text{H}$ distances in the interval 1.7–2.9 Å) gives us some confidence that these quantities are correctly modeled by the VSEC and RODS algorithms used here.

Figure 2 shows the classical barrier, V_{RP} , which is the Born–Oppenheimer potential energy along the reaction path (RP), and the quantal adiabatic ground-state barrier, $\Delta V_{\text{a}}^{\text{G}}$, which is the sum

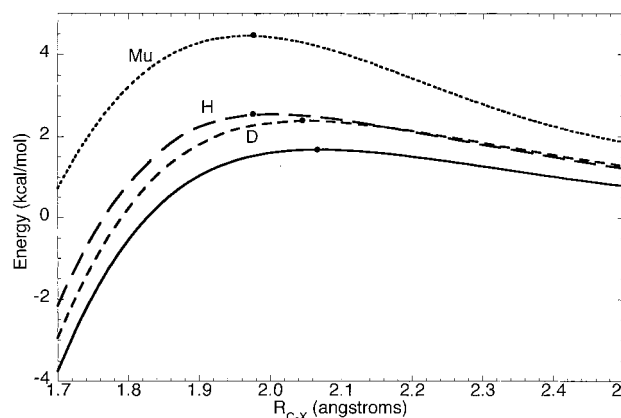


Figure 2. V_{RP} curves (solid lines) and $\Delta V_{\text{a}}^{\text{G}}$ curves for $X = \text{Mu}$ (dotted line), H (long-dashed line), and D (short-dashed line) as functions of the $\text{C}-\text{X}$ distance. The solid circles indicate the location of the maximum of each curve. Although the three reactions have different V_{RP} curves, the differences between them are smaller than the plotting resolution, and thus the three lines appear superimposed.

of V_{RP} and the ZPE relative to its value at reactants, as functions of the $\text{C}-\text{H}$ distance for the three isotopes. This figure allows the reader to compare the widths of the effective barriers for tunneling. The location of the maximum of the $\Delta V_{\text{a}}^{\text{G}}$ curve depends on the isotope and is 0.02–0.09 Å tighter than the saddle point, which has $R_{\text{C}-\text{X}} = 2.07$ Å. The $\Delta V_{\text{a}}^{\text{G}}$ curve corresponds to the free energy of activation profile at 0 K. As the temperature increases, the transition state becomes even tighter for all three of the isotopes. This is one reason conventional transition state theory, which locates the dynamical bottleneck at the maximum of V_{RP} for all of the reactions and temperatures, fails to explain the KIEs. A second reason is the importance of tunneling. The $\Delta V_{\text{a}}^{\text{G}}$ curve is the effective potential for reactive tunneling. Although the barrier is highest for Mu and lowest for D , tunneling through the barrier is an exponentially increasing function of reciprocal mass. The lower mass more than makes up for the higher barrier, leading to the observed $k_{\text{Mu}} > k_{\text{H}} > k_{\text{D}}$. For example, for the D addition the most typical tunneling energy at 230 K is only 0.10 kcal below the maximum of $\Delta V_{\text{a}}^{\text{G}}$, for H it is 0.25 kcal below the maximum, and for Mu it is 3.3 kcal below the maximum. Even Mu atoms with almost zero incident velocity tunnel through the barrier with a probability greater than 10^{-4} , whereas for D atoms the tunneling probability is 10^{-4} for a relative translational energy of 0.9 kcal.

A derived benefit of the good agreement of theory and experiment is that it validates the VSEC prediction of the Born–Oppenheimer barrier height for this prototype reaction, namely 1.7 kcal. Barrier heights for addition reactions have proved to be difficult to calculate directly, and the present estimate should be useful as a benchmark as well as serving as an important first step toward an understanding of more general free-radical addition kinetics.

Acknowledgment. J.C.C. acknowledges the Spanish Ministerio de Educación y Cultura and the Fulbright Commission for a postdoctoral scholarship. This work was supported in part by the U.S. Department of Energy, Office of Basic Energy Sciences.

JA982616I

(21) Liu, Y.-P.; Lynch, G. C.; Truong, T. N.; Lu, D.-h.; Truhlar, D. G.; Garrett, B. C. *J. Am. Chem. Soc.* **1993**, *115*, 2408.

(22) The remaining quantitative discrepancy may be due in large part to anharmonicity, which is neglected here, but which should raise $k_{\text{Mu}}/k_{\text{H}}$.

(23) Lynch, G. C.; Truhlar, D. G.; Brown, F. B.; Zhao, J.-g. *J. Phys. Chem.* **1995**, *99*, 207.